Dynamical Behavior of Poly(2-vinylpyridine) in Solution Studied by ^{13}C Nuclear Magnetic Relaxation

Sapna Ravindranathan and D. N. Sathyanarayana*

Department of Inorganic and Physical Chemistry, Indian Institute of Science, Bangalore 560 012, India

Received July 25, 1994; Revised Manuscript Received November 30, 1994[⊗]

ABSTRACT: The dynamics of poly(2-vinylpyridine) in chloroform solution has been examined by ^{13}C spin−lattice relaxation time and NOE measurements as a function of temperature. The experiments were performed at 50.3 and 100.6 MHz. The backbone carbon relaxation data have been analyzed in terms of six motional models. Among these models, the models which consider conformational transitions and bond librations for the backbone were found to be more successful. Pyridyl ring motion has been modeled as a restricted rotation with the rotational amplitude varying with temperature. The activation energy parameters obtained from the relaxation data of the pyridyl ring carbon have been compared with the energy barrier for ring rotation estimated from conformational energy calculations using the AM1 semiempirical quantum chemical method. The results of the conformational energy calculations support the description of pyridyl ring motion as a restricted rotation.

Introduction

Studies on the dynamics of polymer chains have attracted considerable interest since chain dynamics play an important role in determining the macroscopic properties of polymeric systems. Among the various techniques employed for the study of chain dynamics, nuclear magnetic resonance has proved to be a powerful tool since its selectivity allows a detailed analysis of the motions of the different components of the polymer chain. Studies of chain dynamics in dilute solution have the advantage that it is possible to focus on the internal motions of a single chain because the effects of interchain interactions are minimized.

Nuclear magnetic relaxation processes such as spin−lattice relaxation, spin−spin relaxation, etc. are sensitive to molecular motion. Quantitatively, the relaxation parameters depend on the decay of the orientation autocorrelation function of the individual internuclear vectors. The correlation function embodies the mechanisms and rates of the molecular motions, and obtaining information on this function is the objective of relaxation studies. NMR relaxation parameters (T_1, T_2, NOE) provide information about the correlation functions through their relationship to the spectral density function, which is the Fourier transform of the correlation function. By measuring several relaxation parameters at different resonance frequencies, the spectral density can be sampled discretely at a number of frequencies, thereby gaining some insight into the form of the correlation function.

In polymers, chain connectivity leads to complicated motions and a single exponential correlation function, which was found to be successful in the treatment of dynamics of small molecules, has been found to be inadequate to describe these motions.[1] Currently, there are two equivalent ways of considering this complex situation. One approach is to analyze the experimental data in terms of an empirical distribution of correlation times. In the other approach, a correlation function is derived on the basis of a specific model of the polymer motion, which can then be tested experimentally.

Most of the models for polymer dynamics are based on the conformation transitions of short segments of the backbone. These models have been quite successful because for high molecular weight polymers, the relaxation is governed, to a large extent, by these segmental motions. However, recently, several investigators have emphasized the need to consider motional modes which are more localized, in addition to the segmental motions, in order to understand the differences in the dynamics of C−H vectors at different sites of the chain backbone.[2,3] These highly localized motions have been identified as C−H bond librations.

In the present study, ^{13}C spin−lattice relaxation times (T_1) and nuclear Overhauser enhancements (NOEs) of poly(2-vinylpyridine) (P2VP) have been measured in chloroform solution as a function of temperature at 50 and 100 MHz. In an earlier study by Chachaty et al.[4] ^{13}C T_1 measurements were carried out for P2VP samples of different tacticities and molecular weights at 25 MHz. For a sample of isotactic P2VP in methanol, ^{13}C T_1's were measured as a function of temperature at 25 MHz and the dynamics was interpreted in terms of isotropic rotational diffusion using a single exponential correlation function. This model, however, is inadequate for describing the complex motions which occur in polymer chains. In the present study, we first analyze the experimental results, on the basis of three different motional models, which consider only segmental motions for the polymer chains. We then augument these models by including librational modes of the backbone C−H vectors and compare the results with those of the models based solely on segmental motions. The pyridyl ring motions have been investigated by using composite spectral density functions which include the ring motion along with the description of the backbone motion. The results obtained from the analysis of ring motion are compared with the energy calculations performed on a simple model system.

Experimental Section

P2VP obtained from Aldrich and having a weight average molecular weight of 40 000 was used. The polymer was purified by successive precipitation by hexane from benzene solutions. The samples used for NMR experiments were 10% (wt/vol) in $CDCl_3$.

The ^{13}C nuclear magnetic resonance experiments were carried out on Bruker ACF-200 and Bruker AMX-400 spectrometers operating at 50.3 and 100.6 MHz for the ^{13}C nucleus.

[⊗] Abstract published in *Advance ACS Abstracts,* February 15, 1995.

0024-9297/95/2228-2396$09.00/0

The sample temperature was regulated to ±1 K. The spin–lattice relaxation times were measured by the inversion-recovery technique, which uses a 180°–τ–90° pulse sequence. The delay time between two sequences was 5 times longer than the highest T_1, among those which were to be determined simultaneously. An initial estimate of the T_1 values was obtained from preliminary experiments. A total of 200–300 acquisitions were accumulated for each set of 14 arrayed "τ" values. The T_1 values were determined by fitting the signal intensities as a function of delay time to a three parameter exponential function.[5] Nuclear Overhauser enhancements (NOEs) were measured by comparing ^{13}C signal intensities of the spectra acquired by continuous ^1H decoupling and inverse gated decoupling. In the NOE experiments, delays of 10 times T_1 were used between acquisitions. Experiments were performed on undegassed samples, since the relaxation times of interest are much less than 500 ms, and in such cases, the presence of dissolved oxygen is not expected to contribute significantly to relaxation. The measured T_1's are accurate to within 8%, and the NOEs, accurate to about 15%.

Theoretical Background

Assuming a purely ^{13}C–^1H dipolar relaxation mechanism, the spin–lattice relaxation time, $T_1^{(dd)}$ and nuclear Overhauser enhancement, NOE can be obtained from the following expressions:[6]

$$\frac{1}{T_1^{(dd)}} = Q[J(\omega_H - \omega_C) + 3J(\omega_C) + 6J(\omega_H + \omega_C)] \quad (1)$$

$$Q = \frac{N}{10}\left[\frac{\mu_0 \hbar \gamma_H \gamma_C}{4\pi r^3}\right]^2 \quad (2)$$

$$\mathrm{NOE} = 1 + \frac{\gamma_H}{\gamma_C}\left[\frac{6J(\omega_H + \omega_C) - J(\omega_H - \omega_C)}{J(\omega_H - \omega_C) + 3J(\omega_C) + 6J(\omega_H + \omega_C)}\right] \quad (3)$$

where γ_C and γ_H are the magnetogyric ratios of ^{13}C and ^1H nuclei, respectively, μ_0 is the permeability of vacuum, N is the number of directly bonded protons, r is the C–H internuclear distance, $\hbar = h/2\pi$ where h is Planck's constant, and ω_H and ω_C are the Larmor frequencies of ^1H and ^{13}C, respectively. For the backbone C–H bonds we have used an r value of 1.09 Å obtained from quantum chemistry,[7] and for the pyridyl C–H a value of 1.083 Å[8] obtained from the microwave experimental data for pyridine was used.

The assumption of a purely dipolar relaxation mechanism may not be very accurate for the carbons of the pyridyl ring. At the high magnetic fields used in the present study, the chemical shift anisotropy (CSA) may be an additional relaxation pathway and hence we have included it in the analysis of the relaxation of the ring carbons. On including the CSA contribution, the spin–lattice relaxation rate is given by[9]

$$\frac{1}{T_1} = \frac{1}{T_1^{(dd)}} + \frac{1}{T_1^{(CSA)}} \quad (4)$$

If the chemical shift is axially symmetric, $T_1^{(CSA)}$ is given by[9]

$$\frac{1}{T_1^{(CSA)}} = \frac{2}{15}\omega_C^2(\sigma_\parallel - \sigma_\perp)^2 J(\omega_C) \quad (5)$$

where $\sigma_\parallel$ and $\sigma_\perp$ are the components of the shift tensor, parallel and perpendicular to the symmetry axis. When the CSA mechanism contributes to spin–lattice relaxation in addition to the dipolar mechanism, the expression for NOE becomes[9]

$$\mathrm{NOE} = 1 + \frac{\gamma_H}{\gamma_C}\left[Q\left\{\frac{6J(\omega_H + \omega_C) - J(\omega_H - \omega_C)}{(T_1^{(dd)})^{-1} + (T_1^{(CSA)})^{-1}}\right\}\right] \quad (6)$$

The quantity $(\sigma_\parallel - \sigma_\perp)$ can be obtained from the principal values of the ^{13}C chemical shift tensor using

$$(\sigma_\parallel - \sigma_\perp) = \sigma_{33} - \frac{1}{2}(\sigma_{11} + \sigma_{22}) \quad (7)$$

The calculations have been carried out with $(\sigma_\parallel - \sigma_\perp) = 174$ ppm; obtained from the principal values of the ^{13}C shift tensor of the C_3 carbon of pyridine.[10]

If the shift tensor is axially symmetric, $\sigma_{11} = \sigma_{22}$; however this is not true for the carbons of pyridine.[10] The use of eqs 5 and 6 is thus an approximation but it may be considered adequate for the protonated ring carbons because the contribution of CSA to relaxation would be smaller compared to that of the ^{13}C–^1H dipolar relaxation.

The spectral density function $J(\omega)$ is obtained by the Fourier transformation of the orientation autocorrelation function, $G(t)$.

$$J(\omega) = \frac{1}{2}\int_{-\infty}^{\infty} G(t)e^{i\omega t}\,dt \quad (8)$$

The relaxation times depend on the decay of $G(t)$, and it is governed by the molecular motion. Obtaining the form of $G(t)$ is therefore a decisive step in the interpretation of the relaxation data. For small molecules undergoing isotropic rotational diffusion, $G(t)$ is a single exponential function decaying with a time constant, τ_c, the correlation time.

$$G(t) \approx e^{-t/\tau_c} \quad (9)$$

For polymers, this simple model is unrealistic and hence correlation functions have been derived on the basis of specific motional models. These models are described in the following section.

Models

A polymer chain can undergo a variety of motions such as overall tumbling of the entire chain, conformational rearrangements of the backbone, and motions of pendent groups about an axis within the polymer. In flexible polymers, relaxation is controlled to a large extent by small scale segmental motions which differ widely in their rates and mechanisms. In order to get a comprehensive picture of the polymer dynamics in P2VP, we followed two approaches. In the first approach, the correlation function is expressed as an empirical distribution of correlation times. In this context we have utilized the Cole–Cole and log χ^2 distribution functions. In the second approach, the correlation function is derived on the basis of specific models of the polymer motion. A brief description of the models which we have employed in the analysis of the experimental results is given below.

Cole–Cole Distribution. The Cole–Cole distribution is symmetric and is centered about τ_0. The spectral

density function is given by[11,12]

$$J(\omega) = \frac{1}{2\omega}\left[\frac{\cos\left[(1-\epsilon)\frac{\pi}{2}\right]}{\cosh[\epsilon \ln(\omega\tau_0)] + \sin\left[(1-\epsilon)\frac{\pi}{2}\right]}\right] \quad (10)$$

where ϵ is the width of the distribution and lies in the range $0 \leq \epsilon \leq 1$; the smaller the value of ϵ, the wider the distribution. When ϵ attains its maximum value, this model reduces to the single correlation time model. The parameters in this model are ϵ and the correlation time τ_0.

log χ^2 Distribution. The log χ^2 distribution is asymmetric and skewed toward longer correlation times. The spectral density is given by[13]

$$J(\omega) = \int_0^\infty \frac{\tau_0 F(s)[b^s - 1]\,ds}{(b-1)\{1 + \omega^2\tau_0^2[(b^s-1)/(b-1)]^2\}} \quad (11)$$

where

$$F(s) = \frac{p}{\Gamma(p)}(ps)^{p-1}e^{-ps} \quad (12)$$

The distribution is defined by its width p and the mean correlation time τ_0, which defines the center of the distribution. The Γ function normalizes the distribution to unity. The parameter b describes the logarithmic base and is usually set to 1000. For high values of p ($p \geq 100$), this model also reduces to the single correlation time model.

Jones–Stockmeyer (JS) Model. The JS model is a modification of the diamond lattice model (VJGM) proposed by Valeur et al.[14] The VJGM model is based on three- and four-bond motions (crankshaft motions) which occur in a polymer chain on a tetrahedral lattice. The VJGM correlation function has an extremely slow rate of decay at long times, which is rather unrealistic. The JS model considers three-bond motions, and to overcome the limitation of the VJGM model, the conformational coupling is restricted to a finite chain segment, consequently implying greater local freedom of motion.

In the absence of overall tumbling and internal rotations of pendent groups, the spectral density is given by[15]

$$J(\omega) = \sum_{k=1}^{s} G_k \frac{\tau_k}{1 + \omega^2\tau_k^2} \quad (13)$$

where

$$\tau_k^{-1} = w\lambda_k \quad (14)$$

$$s = (m+1)/2 \quad (15)$$

$$\lambda_k = 4\sin^2\left[\frac{(2k-1)\pi}{2(m+1)}\right] \quad (16)$$

$$G_k = 1/s + (2/s)\sum_{q=1}^{s-1} e^{-\gamma q}\cos[(2k-1)\pi q/2s] \quad (17)$$

and

$$\gamma = \ln 9 \quad (18)$$

The parameter w is the rate of occurrence of a three-bond jump, usually expressed in terms of the harmonic mean correlation time τ_h which defines the time scale of the segmental motion, $\tau_h = (2w)^{-1}$. The breadth of the distribution of correlation times is characterized by the number of bonds m involved in the cooperative motion. The quantity $(2m-1)$ represents the chain segment expressed in bonds that are coupled to the central three-bond unit, and no correlated motions are assumed outside the segment.

Hall–Weber–Helfand (HWH) Model. The HWH model takes into account pair transitions involving simultaneous rotations about two bonds and isolated transitions which involve rotations about one bond. The spectral density is given by[2,16]

$$J(\omega) = Re\left[\frac{1}{(\alpha + i\beta)^{1/2}}\right] \quad (19)$$

where

$$\alpha = \frac{1}{\tau_0^2} + \frac{2}{\tau_0\tau_1} - \omega^2 \quad (20)$$

and

$$\beta = -2\omega\left[\frac{1}{\tau_0} + \frac{1}{\tau_1}\right] \quad (21)$$

Here τ_1 and τ_0 are the correlation times for the pair and isolated transitions, respectively.

Librational Motions. Recently, there has been considerable emphasis in the literature on the necessity to consider two classes of motions occurring on well-separated time scales for a better description of the backbone motion. The HWH model was found to underestimate the value of T_1 at the minimum and it also failed to account for the different local dynamics observed at different carbons of the polymer chain.

The Dejean, Laupretre, Mounnerie (DLM) model[2] which is a modification of the HWH model, overcomes the deficiencies of the HWH model by superimposing an additional independent motion on the backbone rearrangement of the HWH model. The additional motion involves librations of the C–H vectors of the backbone with a correlation time, τ_l. The resulting spectral density expression is given by

$$J(\omega) = \frac{1-f}{(\alpha + i\beta)^{1/2}} + \frac{f\tau_l}{1 + \omega^2\tau_l^2} \quad (22)$$

Gisser et al.[3] have introduced librational motion in the Cole–Cole distribution and single exponential correlation functions. The models which include librations were found to be more successful in describing the experimental relaxation data. Following the approach of Dejean et al.[2] we have appended the librational motion to the JS model and the Cole–Cole distribution and the spectral density expressions in the two models are respectively

$$J(\omega) = (1-f)\sum_{k=1}^{s} G_k \frac{\tau_k}{1 + \omega^2\tau_k^2} + \frac{f\tau_l}{1 + \omega^2\tau_l^2} \quad (23)$$

and

$$J(\omega) = (1-f)\frac{1}{2\omega}\left[\frac{\cos\left[(1-\epsilon)\frac{\pi}{2}\right]}{\cosh[\epsilon \ln(\omega\tau_0)] + \sin\left[(1-\epsilon)\frac{\pi}{2}\right]}\right] + \frac{f\tau_1}{1+\omega^2\tau_1^2} \quad (24)$$

Inclusion of librational motion introduces additional parameters into the models, namely the ratio of segmental motion correlation times to that of libration and f, the relative weight of the librational component.

Numerical Calculations

Relaxation data were analyzed by using the spectral density functions discussed in the previous section. In order to obtain a fit of T_1 as a function of temperature, we have introduced the temperature dependence of correlation times in the spectral density expressions.

Helfand[17] has applied Kramer's theory[18] for the diffusion of a particle over a potential barrier to conformational transitions in a polymer. According to this theory, the correlation time τ, for a conformational transition involving an energy barrier E_a, is written as,

$$\tau = Ae^{E_a/RT} \quad (25)$$

where $A = \eta C$, η being the viscosity and C, a molecular constant. In the calculations, the activation energy, E_a and the pre-exponential factor, A, were taken as adjustable parameters.

Temperature dependent T_1 values at both the frequencies were fitted simultaneously. For the Cole–Cole, log χ^2, JS, and HWH models, the experimental T_1 values for the methine carbon at different temperatures were used as the input data. The width parameters in these models (ϵ, p, m, and τ_0/τ_1) were varied manually, and the values of A and E_a which provided the best fit were obtained. Fitting was achieved by minimizing the sum of the squares of the deviations between the calculated and experimental values using a simplex routine. The parameters thus obtained were used to predict the relaxation data of the methylene carbon.

For the more complicated models, namely DLM, modified JS, and modified Cole–Cole involving librations parameters, A, E_a, and f were included in the fitting procedure and the remaining parameters were adjusted manually. The experimental data corresponding to the methine carbon were utilized to obtain the model parameters. These parameters were held constant while the values of f giving the best fit to the methylene carbon data were determined. The deviations between the calculated and experimental quantities are expressed as the mean square of relative deviations denoted as d. The conformational energy calculations have been carried out by the AM1 method[19] as implemented in the Gaussian 92 program package.[20]

Results

Isotactic and atactic P2VP have been studied by NMR and the spectral features are well documented in the literature.[21,22] The proton NMR spectrum of the sample under investigation indicated random tacticity. Following the approach of the earlier investigators,[21] we have estimated the probability of isotactic addition, P_m, to be 0.48. The labeling of the carbon atoms in the repeating unit of P2VP is indicated below.

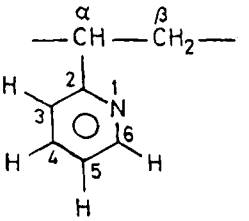

In Table 1 we summarize the ^{13}C T_1 values and NOEs for the backbone carbon atoms and the C_3, C_4, and C_5 carbons of the pyridyl moiety. The experimental data display the following features. With increasing temperature, the T_1 values of the backbone carbons reach a minimum and then increase. The T_1 values are higher at higher magnetic field in the entire temperature range of study. The NOE values decrease with increasing magnetic field and are well below the limiting value of 3.0 in the entire temperature range at both the fields. The latter two observations suggest that the motional characteristics are far below the extreme narrowing limit in the whole temperature range studied for both the fields, and further it implies that a single exponential correlation function, that is, isotropic motion, is inadequate to account for these relaxation data. Another important observation is that the ratio of T_1 values of the CH group to the CH_2 group, i.e., $T_1(CH)/T_1(CH_2)$, is approximately 1.8 ± 0.1 throughout the temperature range. This value is different from 2, which is expected from the number of directly bonded protons and suggests that the C–H internuclear vectors associated with the CH and CH_2 groups may be subjected to different local motions.

The relaxation times of C_3 and C_4 carbons are similar at both the fields in the entire temperature range of study and they are higher than that of the methine carbon, especially at higher temperatures. On the other hand, the relaxation times for the C_5 carbon are lower than those of C_3 and C_4 carbons but they are comparable to those of the methine carbon, especially at the higher field. The observations suggest that the pyridyl ring motion could be modeled as a rotation about the C_2–C_5 axis. As a consequence of such a motion, the C_3–H and C_4–H internuclear vector would undergo reorientation whereas the C_5–H vector would be little influenced and the relaxation of the latter would largely be determined by the backbone rearrangements.

Discussion

In modeling the dynamics of P2VP, we consider two types of motions: (i) segmental rearrangments of the backbone and (ii) motion of the pyridyl group. A third type of motion which might contribute to relaxation is the overall tumbling of the polymer chain. The latter motion of the polymer chain can compete with local segmental motions if the correlation time is of the same order as that of the segmental motions or less. The correlation time for overall tumbling motion, τ_R, can be obtained from the hydrodynamic equation[23,24]

$$\tau_R = 2M[\eta]\eta_0/3RT \quad (26)$$

where M is the molecular weight, $[\eta]$ is the intrinsic viscosity of the polymer solution, and η_0 is the solvent viscosity.

Earlier studies of T_1 as a function of molecular weight for P2VP have shown that when the degree of polym-

Table 1. Experimental Carbon-13 Spin–Lattice Relaxation Times (ms) and NOE[a] of Protonated Carbons of P2VP as a Function of Temperature at Two Magnetic Fields

	backbone carbons				pyridyl ring carbons					
	CH		CH_2		C_3		C_4		C_5	
temp, K	50.3 MHz	100.6 MHz	50.3 MHz	100.6 MHz	50.3 MHz	100.6 MHz	50.3 MHz	100.6 MHz	50.3 MHz	100.6 MHz
248	131 (1.53)	277 (1.43)	67 (1.53)	161 (1.36)	147 (1.45)	268 (1.35)	145 (1.47)	263 (1.39)	137 (1.44)	256 (1.28)
263	111 (1.56)	249 (1.49)	58 (1.67)	136 (1.45)	131 (1.56)	248 (1.43)	136 (1.5)	246 (1.45)	128 (1.5)	248 (1.41)
283	113 (1.77)	237 (1.57)	63 (1.8)	125 (1.58)	139 (1.75)	253 (1.51)	137 (1.69)	244 (1.47)	129 (1.71)	234 (1.48)
296	126 (1.85)	240 (1.66)	70 (2.0)	128 (1.71)	157 (1.83)	258 (1.89)	157 (1.87)	249 (1.77)	142 (1.92)	240 (1.77)
308	144 (2.13)	251 (1.84)	80 (2.14)	135 (1.84)	189 (2.1)	263 (1.92)	191 (2.07)	260 (1.85)	165 (2.06)	246 (1.84)
318	164 (2.29)	260 (2.04)	92 (2.29)	148 (1.89)	227 (2.23)	279 (1.95)	223 (2.3)	275 (1.89)	202 (2.18)	264 (1.87)

[a] Values in parentheses.

Table 2. Simulation Parameters for Methine Carbon T_1 of P2VP

model	width[a]	τ_s/τ_l[b]	f	E_a, kJ/mol	$10^{13}A$, s	10^3d
Cole–Cole	0.69			20.3	1.75	2.10
log χ^2	19			22.3	0.846	1.99
JS	7			26.7	0.0751	2.76
HWH	20			27.4	0.0709	7.64
modified Cole–Cole	0.70	10	0.470	21.7	5.4	2.62
		(100	0.0169	20.1	2.0)[c]	1.73
		1000	0.0166	19.9	2.2	1.99
		10000	0.0165	20.0	2.1	2.01
modified JS	5	10	0.560	20.9	8.12	1.73
		100	0.0787	24.0	0.225	1.46
		(130	0.078	23.9	0.229)[c]	1.46
		1000	0.077	23.8	0.241	1.46
		10000	0.077	23.7	0.246	1.46
DLM	8	10	0.439	24.7	0.841	1.26
		(100	0.190	18.5	3.95)[c]	2.35
		1000	0.183	18.1	4.50	2.35
		10000	0.182	18.1	4.53	2.41

[a] Width refers to ϵ, p, m, or τ_0/τ_l. [b] τ_s/τ_l corresponds to τ_0/τ_l, τ_h/τ_l, and τ_1/τ_l for modified Cole–Cole, modified JS, and DLM models, respectively. [c] Values in parentheses indicates the parameter set used to plot T_1 and the NOE of the methine carbon as a function of temperature.

Table 3. Simulation Parameters[a] for Methylene Carbon T_1 of P2VP

model	τ_s/τ_l[b]	f	10^3d
Cole–Cole			7.18
log χ^2			7.54
JS			10.90
HWH			18.80
modified Cole–Cole	10	0.391	8.21
	(100	0.113)[c]	2.51
	1000	0.107	2.42
	10000	0.106	2.35
modified JS	10	0.484	7.25
	100	0.165	2.68
	(130	0.165)[c]	2.66
	1000	0.161	2.55
	10000	0.161	2.56
DLM	10	0.431	8.44
	(100	0.267)[c]	2.86
	1000	0.258	2.76
	10000	0.257	2.75

[a] Values of E_a and A are the same as for the methine carbon. [b] τ_s/τ_l corresponds to τ_0/τ_l, τ_h/τ_l, and τ_1/τ_l for modified Cole–Cole, modified JS and, DLM models, respectively. [c] Values in parentheses indicate the parameter set used to plot T_1 and the NOE of the methylene carbon as a function of temperature.

erization exceeds 100, T_1 becomes independent of the molecular weight.[4] It implies that when the degree of polymerization exceeds 100, relaxation is largely controlled by the segmental motions of the backbone. The polymer sample used in the present study, has a degree of polymerization approximately 380 and hence we do not expect any significant contribution to relaxation from the overall tumbling process.

In the present study the segmental motions have been modeled by the Cole–Cole distribution, log χ^2 distribution, JS, and HWH correlation functions. The effect of the inclusion of librational motion has been examined using the DLM model and by the Cole–Cole and JS models by modifying the respective spectral density functions. Motion of the pyridyl ring has been modeled as a restricted rotation. In the following discussion, we have evaluated the models in their ability to describe local motions of the chain and the description of pyridyl ring motion as a restricted rotation has been supported by conformational energy calculations.

(i) Segmental Motion of the Main Chain. We first analyze the experimentally observed relaxation data for the methine and the methylene carbons of the backbone using the Cole–Cole, log χ^2, JS, and HWH correlation functions. The parameters which give the best fit of the methine carbon T_1 data to the above models are given in Table 2. The Cole–Cole and log χ^2 models reproduce the experimental data very well and the performance of both the models are comparable, as seen from the d values included in Table 2. The JS and HWH models on the other hand, predict minima which are much lower than the experimentally observed minima. The underestimation of the T_1 minima when analyzed by the HWH model has also been noted for other polymers.[2,25–28] The width parameters in these models can be expressed as a function of temperature, and it is expected that as the extreme narrowing limit is approached, the width parameters attain a limiting value for which the correlation function becomes equivalent to the single exponential function. However, in the present case, no appreciable changes were observed in the best fit width parameter values even when the relaxation data at each temperature were fitted separately. We therefore conclude that in the temperature range under study, the width parameter does not change and hence it is not expressed as a function of temperature in the fitting procedure.

We now consider the relaxation times of the methylene carbon. If the reorientation of the backbone C–H vectors is solely due to the segmental motion, the parameters obtained for the methine carbon should also be able to account for the relaxation data of the methylene carbon. The calculated T_1 values for the methylene carbon deviate significantly from the experiment for all the models, as is evident from the d values given in Table 3. In the entire temperature range, the calculated values are less than the experimental values. This indicates that the reorientation of the C–H vectors is not entirely determined by the segmental motions.

Recently, C–H bond libration has been used successfully by several authors to obtain a better description of the experimental features. We have employed the DLM model and the modified Cole–Cole and JS functions which include librations in order to examine the

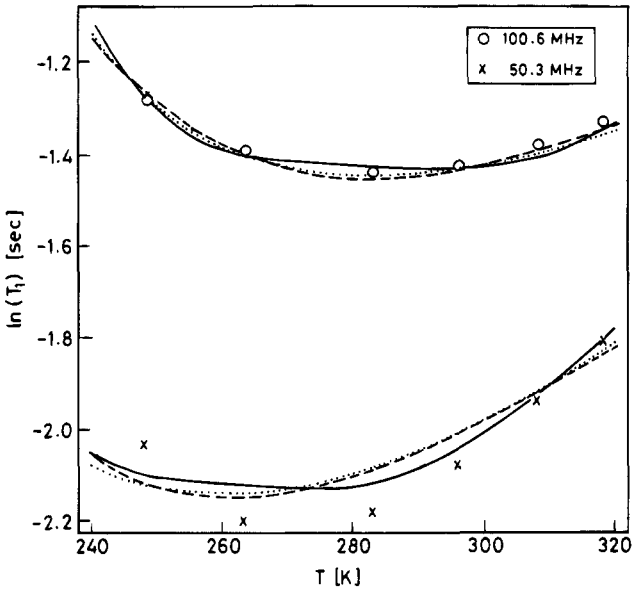

Figure 1. Temperature dependence of T_1 for the methine carbon of P2VP in $CDCl_3$. Solid, dashed, and dotted lines represent results obtained using the modified JS, modified Cole–Cole, and DLM correlation functions, respectively. The points are experimental T_1 values obtained at two Larmor frequencies.

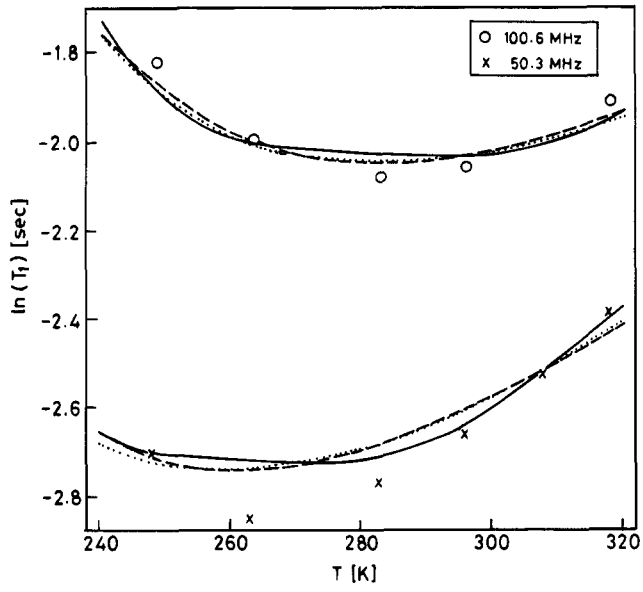

Figure 2. Temperature dependence of T_1 for the methylene carbon of P2VP in $CDCl_3$. Solid, dashed, and dotted lines represent results obtained using the modified JS, modified Cole–Cole, and DLM correlation functions, respectively. The points are experimental T_1 values obtained at two Larmor frequencies.

effect of this additional mode on the relaxation behavior. With inclusion of libration, we have two additional parameters, namely, the ratio of the correlation time for segmental motion to that of libration, and a weight factor f, which serves as a measure of the contribution of the two types of motions.

The best fit of T_1 versus T curves for the methine carbon, calculated on the basis of the modified Cole–Cole, modified JS, and DLM models are shown in Figure 1, and the model parameters are included in Table 2. The T_1 values obtained from the modified Cole–Cole model are very close to the values obtained from the Cole–Cole model at all temperatures; the difference is about 1%. An examination of Table 2 shows that the d values for both the models are nearly the same. The inclusion of the librational mode of the C–H vector of the methine group in the Cole–Cole model does not change its predicted relaxation times. Examination of the best fit parameters given in Table 2 reveals that the weight factor f, associated with the librational mode, is negligibly small (0.0169). In the modified model, two types of motional modes contribute to the decay of the orientation correlation function of the C–H vector, namely, the segmental motion of the backbone and the librational motion of the C–H vector. A very small value obtained for the weight factor implies that the librational mode contributes negligibly (about 2%) to the decay of the correlation function. A major contribution therefore comes from the backbone rearrangements.

The modified JS and DLM models on the other hand show a substantial improvement over the results obtained from calculations based on the JS and HWH models, respectively. The inclusion of the librational mode in the latter models leads to prediction of T_1 values in better agreement with experiment, as indicated by a comparison of the d values given in Table 2. The values of the weight factor obtained for the modified JS and DLM models imply that the contribution from the librational modes to the decay of the correlation function is about 8% and 19%, respectively.

Figure 2 shows the best fit T_1 versus T curves for the methylene carbon based on the modified Cole–Cole, modified JS, and DLM models, and the model parameters are given in Table 3. The inclusion of the librational mode raises the T_1 minimum and leads to improved agreement with experimental values for all the three models. Table 3 shows significant lowering of d values for the models which include libration. The contribution from the librations of the C–H vector of the methylene group to the decay of the correlation function is approximately 11%, 17%, and 27%, respectively, for the modified Cole–Cole, modified JS, and DLM models. A notable common feature in these models is that the value of the weight factor is less for the methine carbon than that for the methylene carbon. The smaller value for the methine group indicates greater steric hindrance to the librational motion of the C–H vector of the methine group relative to that in the methylene group. The methine carbon has a directly attached pyridyl group, which owing to its size, may physically hinder the librational motion. This observation agrees with the earlier findings for other polymers.[2,25,26,28,29]

The amplitude of librational motion can be estimated from the parameter, f, in conjunction with Howarth's restricted rotation model.[30] In this model, libration is described as the motion of the C–H vector inside a cone of half-angle θ, the axis of the cone being the rest position of the C–H bond. The angle θ can be estimated from the expression[30]

$$1 - f = \left[\frac{\cos\theta - \cos^3\theta}{2(1 - \cos\theta)}\right]^2 \qquad (27)$$

The conic half-angles estimated for the three models are different. From the modified Cole–Cole model, the calculated values of θ for the CH and CH_2 are 6.1 and 16.1°, respectively, and the corresponding values based on the DLM and the modified JS models are 21.3, 25.7° and 13.3, 19.7°. The librational mode influences the calculated T_1 values through two factors, namely, the

correlation time for libration and the quantity f which is related to the amplitude of libration. Dejean et al.[2] have examined the effect of these two factors on the calculated T_1 values. The librational correlation time shows a noticeable influence only on the higher correlation time side of the T_1 minimum. The T_1 value at the minimum is directly proportional to $1/(1-f)$ and hence the height of the T_1 minimum is highly dependent on the amplitude of the librational mode.

In our analysis of the T_1 data we have observed that among the models which does not include libration, the HWH model predicts minima far below the experimental values for both methine and methylene carbons. The JS model shows a slight improvement over the HWH model and in the case of the Cole–Cole model, a significant lowering of T_1 minimum is observed only for the methylene carbon. In fact, the extent of deviation from the experimental minimum parallels the trend observed in the d values given in Tables 2 and 3. The inclusion of the librational mode leads to raised T_1 minima closer to the experimental observation and the amplitude of the librational mode is the deciding factor. The models for which the lowering of T_1 minimum is greater require a higher librational amplitude to account for the experimentally observed minimum.

By employing the models which include libration, it is rather difficult to determine accurately the ratio of the correlation time for segmental motion to that of libration. As noted from Tables 2 and 3, varying this ratio from 10 to 100 leads to significant improvement in the calculated relaxation parameters for all the models. A further change from 100 to 10 000 produces negligible variation in the calculated values, as seen from the deviations (d). Beyond a value of 100, the values of f, A, and E_a are also observed to be almost stable.

As independent source for testing the correlation function is the NOE.[31] The parameters obtained from the various models can be utilized to predict the NOE as a function of temperature. The single exponential correlation function predicts NOE to be dependent on correlation time only in the region of T_1 minimum and reaches the asymptotic limits of 2.988 and 1.154 for $\omega_c\tau_c \ll 1$ and $\omega_c\tau_c \gg 1$, respectively.[6] Examination of the experimental NOE values given in Table 1 indicates that for both methine and methylene carbons, the NOE increases gradually at lower temperatures, followed by a sharp increase. However for both fields, the NOE does not reach its limiting value of 2.988.

The parameters obtained from the modified Cole–Cole, modified JS and DLM models by fitting the T_1 data have been employed to predict NOE as a function of temperature. The predictions of these models for methine and methylene carbons are shown in Figures 3 and 4, respectively. The modified JS model predicts a sharp rise in NOE with temperature; this increase is however at a lower temperature than that observed experimentally. Although this model predicts an NOE versus temperature curve which is sigmoidal in shape, the increase in NOE is not continuous. After an initial increase, the curve levels off and then begins to increase further. This feature is not observed experimentally.

The DLM and modified Cole–Cole models on the other hand, reproduce the experimental features correctly. These models like the single exponential correlation function, predict the NOE to be independent of temperature at temperatures below the T_1 minimum.

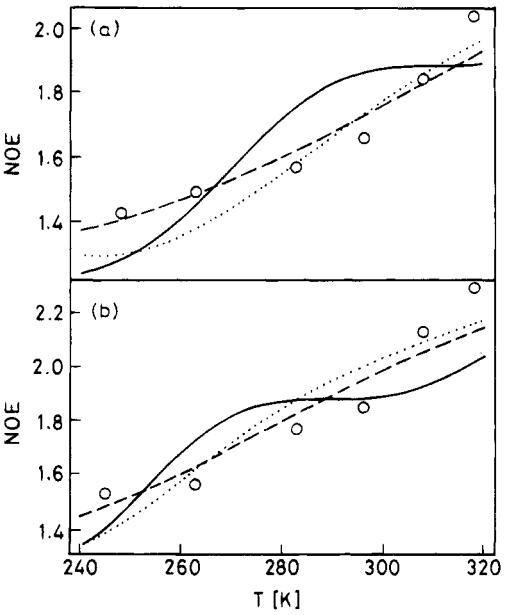

Figure 3. Temperature dependence of NOE for the methine carbon at (a) 100.6 MHz and (b) 50.3 MHz. Solid, dashed, and dotted lines represent the predictions of the modified JS, modified Cole–Cole, and DLM correlation functions, respectively. The points are experimental NOE values. The model parameters obtained by fitting to the experimental T_1 data are given in Table 2.

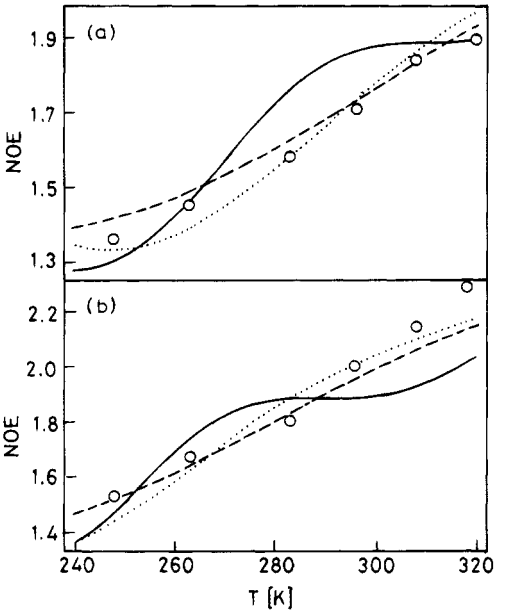

Figure 4. Temperature dependence of NOE for the methylene carbon at (a) 100.6 MHz and (b) 50.3 MHz. Solid, dashed, and dotted lines represent the predictions of the modified JS, modified Cole–Cole, and DLM correlation functions, respectively. The points are experimental NOE values. The model parameters obtained by fitting to the experimental T_1 data are given in Table 3.

This feature is disernible from the curves calculated for the higher field.

The three librational models give good fittings for the T_1 values of the methine and the methylene carbons. For further comparison we consider the modified JS and DLM models. Even though both models give similar fit to the T_1 values of the backbone carbons, the modified JS model fails to reproduce the experimental NOE satisfactorily. On the basis of the DLM model, the activation energy calculated, is 18.5 kJ/mol. The ob-

served activation energy may be written as[18,32]

$$E_a = E_\eta + E^* \tag{28}$$

where E_η is the activation energy for solvent viscosity and E^* is the potential barrier for the conformational transitions of the backbone. From a plot of ln η versus $1/T$, where η is the viscosity of the solvent (chloroform), E_η was found to be 7.4 kJ/mol.[33] It leads to a value of 11.1 kJ/mol for E^*.

However, it should be noted that the activation barrier for conformational transitions obtained by the above method may not be very accurate. Recently, Glowinkowski et al.[33] have shown that Kramer's theory breaks down when the time scales for the polymer and solvent motions are not cleanly separable. This is particularly true in solvents of high viscosity; where the time scales for the polymer and solvent motions are very similar. In P2VP, for the temperature range of study, the correlation times for the conformational transitions range from about 3×10^{-9} to 4×10^{-10} s and the motional characteristics are far from the extreme narrowing limit. In this particular situation we can assume that the time scales for the polymer and solvent motions are quite different and the use of Kramer's theory may not lead to very large errors. For better estimates, it is necessary to investigate the dynamics in solvents of different viscosities. The estimated activation energy may be used to obtain some insight into the nature of the backbone motion.

Helfand[17] has classified polymer conformational transitions according to the position of the chain ends attached to a segment undergoing the transition. Type 1* motion is a crankshaft motion involving rotation about two collinear bonds, leaving the positions of the chain ends unchanged. In type 2* motion the conformational transition results in a translational motion of the chain ends. The observed activation energy of 11 kJ/mol is consistent with a single bond rotation. This implies that type 2* motions are more likely in P2VP, since a type 1* motion would involve a higher energy barrier due to simultaneous rotations about two bonds.

(ii) Anisotropic Motion of the Pyridyl Ring. Examination of the experimental data given in Table 1 shows that the T_1 values for the ring carbons are comparable to that of the methine carbon of the backbone. It suggests that the pyridyl ring does not have much motional freedom relative to the backbone. For a quantitative analysis of the experimental data of the side group nuclei, the spectral density expression has to be modified to account for the additional motions of the side group.

For modeling the pyridyl group motion we have used the following approach. The relaxation of the pyridyl ring carbons is governed by the reorientation of the C−H vectors of the pyridyl group, which results from the backbone motions and ring motions. The backbone motion has been shown to be best described by the motional models which include libration. In these models, motions occurring on different time scales are involved in the motional modes of the backbone. These are the conformational transitions which are expressed by the JS and HWH functions, and the librations of the backbone C−H vectors. The librational motion is not expected to influence the relaxation of the pyridyl ring nuclei since it does not result in the reorientation of the ring C−H vectors. In modeling the pyridyl motion, we therefore do not include the librational term which occurs in the modified JS and DLM models. However, the parameters involved in the description of the conformational transitions are fixed by the best fit values obtained for the backbone carbon relaxation data based on the modified JS and DLM models. This approach is similar to the treatment of motion in polycarbonates[34] where the backbone motion has been shown to involve conformational transitions as well as phenyl ring rotations. However, only the former is included in the description of rotations of the methyl side chain.

Attempts to model the ring rotations using stochastic diffusion processes or jumps in a 2-fold potential barrier proposed by Jones[35] were unsuccessful. We have followed the approach proposed by Ghesquiere et al.[36] in which the motion of the pyridyl ring about the C_2-C_5 axis is considered as oscillations of small amplitude. Other investigators have adopted a similar approach for describing side group motion by treating it as a restricted rotation.[37,38] The composite spectral density which includes pyridyl rotation is given by[36]

$$J(\omega) = \frac{3}{8}\left\{\left[\frac{2}{3}(1 - 3\cos^2\gamma)^2 + \sin^2 2\gamma(1 + \cos\alpha) + \sin^4\gamma(1 + \cos 2\alpha)\right]J(\tau_b,\omega) + [\sin^2 2\gamma(1 - \cos\alpha) + \sin^4\gamma(1 - \cos 2\alpha)]J(\tau_t,\omega)\right\} \tag{29}$$

where γ denotes the angle between the internuclear vector and the axis of rotation and α is the angular amplitude of the oscillation. When the segmental motion is described by the JS model, $J(\tau_b,\omega)$ is given by the expression (13) with $\tau_b = \tau_k$, and for the HWH description of the segmental motion, $J(\tau_b,\omega)$ is given by eq 19 with $\tau_b = \tau_0$. $J(\tau_t,\omega)$ is obtained by replacing τ_k or τ_0 by τ_t in the above expression and τ_t is defined by

$$\tau_t^{-1} = \tau_b^{-1} + \tau_{ir}^{-1} \tag{30}$$

where τ_{ir} is the correlation time for the ring rotation. When the angular amplitude α is 180°, the above expression becomes the same as the 2-fold jump proposed by Jones. In the following, the composite expression in which the segmental motion is described by the JS function will be referred to as ring model 1, and when the segmental motion is described by the HWH function, it will be referred to as ring model 2.

The best fit T_1 versus T curves for the C_3 carbon based on the above models are shown in Figure 5 and the model parameters are given in Table 4. Both the models show good agreement with the experimental data. In the fitting procedure the angular amplitude of the ring rotation was allowed to vary with temperature; the dependence is of the form

$$\alpha = CT^{1/2} \tag{31}$$

A similar temperature dependence for the amplitude of the phenyl group motion has been adopted by Gronski[38] for modeling the restricted internal rotation of the side groups. For ring model 1, α was found to vary from 42 to 48° in the temperature range of study. Using ring model 2, α values were found to range from 49 to 55°. The α values obtained by both the models indicate the ring rotation to be highly restricted, and it involves small angular oscillations. Though the motional amplitude is limited, the motion is faster than the backbone rearrangements, as is evident from a comparison of the correlation times for the segmental and ring motions given in Table 5. The restricted rotational amplitude

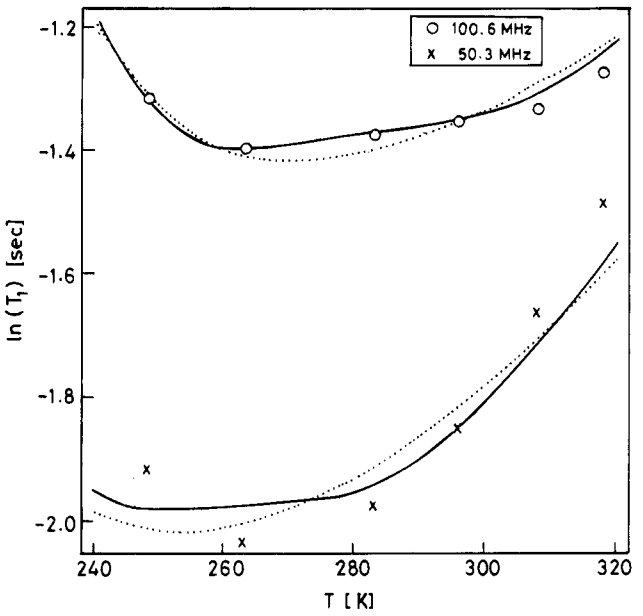

Figure 5. Temperature dependence of T_1 for the C_3 carbon of the pyridyl ring. Solid and dotted lines represent results obtained based on the ring models 1 and 2, respectively. The points are the experimental T_1 values obtained at two Larmor frequencies.

Table 4. Simulation Parameters for C_3 T_1

model	E_a, kJ/mol	$10^{13}A$, s	C	10^3d
ring model 1	13.9	0.383	2.67	1.8
ring model 2	14.6	0.178	3.09	2.8

Table 5. Correlation Times for Pyridyl Ring Rotation of P2VP

temp, K	modified JS[a] $10^9\tau_h$, s	ring model 1 $10^{11}\tau_{ir}$, s	DLM[a] $10^9\tau_1$, s	ring model 2 $10^{11}\tau_{ir}$, s
248	2.471	3.282	3.134	2.131
263	1.276	2.233	1.878	1.423
283	0.590	1.424	1.033	0.887
296	0.378	1.098	0.731	0.675
308	0.259	0.881	0.545	0.536
318	0.193	0.742	0.434	0.448

[a] Correlation times for cooperative segmental motions are included for comparison.

may be due to steric hindrance caused by the presence of nearby bulky pyridyl groups.

The predicted NOE as a function of temperature for the C_3 carbon, based on the two models, is shown in Figure 6. As noted for the calculated NOEs for the backbone carbons, ring model 1 predicts a leveling-off of the NOE which is not observed experimentally. Ring model 2, on the other hand, is more successful in reproducing the experimental features observed for the NOE. At the higher field, the deviation of the calculated values from experimental values is more but it remains within 10% for most of the temperature range considered. A comparison of the performance of the two models shows that ring model 2 reproduces the experimental features satisfactorily. Ring model 2 yields an activation energy of 14.6 kJ/mol. After the energy barrier due to solvent viscosity is subtracted, the potential barrier for the ring rotation is 7.2 kJ/mol.

For a more detailed study of the ring motion, it is necessary to have an estimate of the energy barrier involved in the pendent group motion by independent means. We have carried out conformational energy calculations on the following model which was chosen

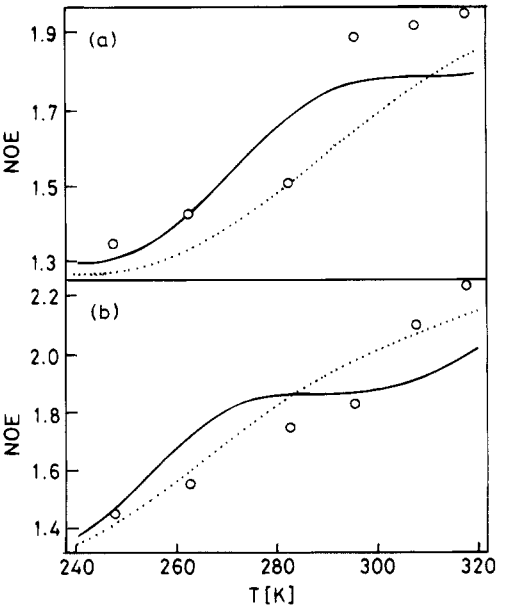

Figure 6. Temperature dependence of NOE for the C_3 carbon of the pyridyl ring at (a) 100.6 MHz and (b) 50.3 MHz. Solid and dotted lines represent predictions of ring models 1 and 2, respectively. The model parameters obtained by fitting to experimental T_1 data are given in Table 4.

to represent the polymer under investigation.

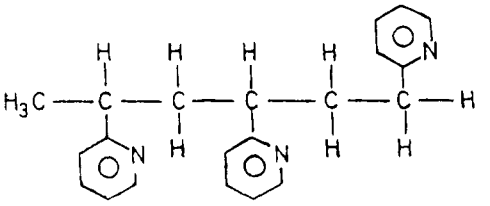

The structural parameters obtained from the geometry of ethylpyridine optimized by the SCF/3-21G method of ab initio quantum chemistry were used to build up the above model. The structure of the model compound was optimized using the semiempirical quantum chemical method, AM1. During optimization, the bond lengths were held constant and the interbond angles and torsional angles were allowed to vary. The optimized structure was found to have TTGTT conformation for the backbone, and the pyridyl ring is oriented perpendicular to the backbone with the ring nitrogen pointing away from the methine hydrogen.

All the energy calculations were performed using the AM1 method. In order to generate the potential energy curve for the pyridyl ring motion, the rotation angle, ϕ, of the central pyridyl ring was varied in increments of 10°. At each step, all the bond angles and torsional angles were optimized in order to avoid possible overestimation of the potential barrier of interest which might result otherwise. The bond lengths, however, were kept constant, since it is very unlikely that the bond length changes appreciably, as a result of the ring rotation. The potential energy as a function of the rotation angle, ϕ, is given in Figure 7. Examination of the potential energy curve shows that an activation barrier of approximately 23 kJ/mol should be overcome for a complete rotation through 180° of the pyridyl ring. Interestingly, Ghesquiere et al.[36] have also reported an activation barrier of about 21 kJ/mol for the pyridyl ring motion in poly(4-vinylpyridine). Such a high energy barrier suggests that the pyridyl ring motion must be

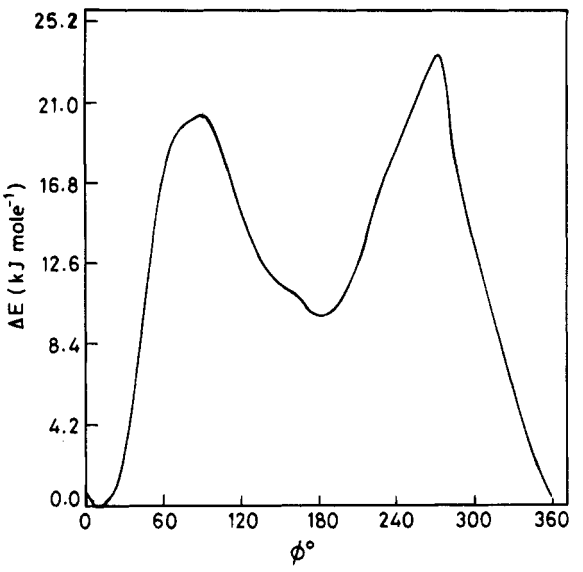

Figure 7. Energy barrier to internal rotation of the pyridyl ring calculated using the semiempirical quantum chemical method, AM1.

of limited amplitude. Based on the analysis of the ring carbon data, using ring model 2, the amplitude of ring rotation has been estimated to vary from 49 to 55° in the entire temperature range of study and it involves an energy of about 7.2 kJ/mol. Energy of this magnitude corresponds to angular amplitudes of the order of 40 to 43° in the potential energy curve. The rotational amplitudes estimated from conformational energy calculations are comparable to those obtained from the experimental relaxation data.

Conclusion

The ^{13}C relaxation data for the backbone and ring carbons of P2VP have been analyzed by different motional models for the polymer chains. Models which consider motions on two different time scales for a complete description of the backbone motion were found to be more successful in the analysis of the relaxation data. These motions include conformational transitions of short segments of the backbone and the C−H bond librations. The best fit to the experimental relaxation times was obtained from the DLM model. The libration amplitude is lower for the C−H vectors of the methine carbon relative to that of the methylene carbon due to steric hindrance resulting from the presence of the bulky pyridyl group on the methine carbon. The ring carbon relaxation data have been interpreted satisfactorily by considering the ring motion as rotations of restricted amplitude. It was confirmed by the conformational energy calculations carried out on a model compound, which showed a very high activation barrier for 180° rotations of the pyridyl ring. In the temperature range of study, the rotational amplitude of the pyridyl ring varies from 49 to 55°. The rotational amplitude estimated from the conformational energy calculations was found to be reasonably close to the value obtained from the experimental relaxation data.

Acknowledgment. The 400 MHz NMR experiments were carried out at the Sophisticated Instruments Facility, Indian Institute of Science. We thank the staff for assistance. S.R. is greatly thankful to the Council of Scientific and Industrial Research (CSIR), India, for a fellowship.

References and Notes

(1) Heatley, F. *Annu. Rep. NMR Spectrosc.* **1986**, *17*, 179.
(2) Dejean de la batie, R.; Laupretre, F.; Monnerie, L. *Macromolecules* **1988**, *21*, 2045.
(3) Gisser, D. J.; Glowinkowski, S.; Ediger, M. D. *Macromolecules* **1991**, *24*, 4270.
(4) Chachaty, C.; Forchioni, A.; Ronfard-Haret, J. *Makromol. Chem.* **1973**, *173*, 213.
(5) Sass, M.; Ziessow, D. *J. Magn. Reson.* **1977**, *25*, 263.
(6) Doddrell, D.; Glushko, V.; Allerhand, A. *J. Chem. Phys.* **1972**, *56*, 3683.
(7) Pople, J. A.; Gordan, M. S. *J. Am. Chem. Soc.* **1967**, *89*, 4253.
(8) Mata, F.; Quintana, M. J.; Sorensen, G. O. *J. Mol. Struct.* **1977**, *42*, 1.
(9) Lyerla, J. R.; Levy, G. C. *Top. Carbon-13 NMR Spectrosc.* **1974**, *1*, 79.
(10) Parhami, P.; Fung, B. M. *J. Am. Chem. Soc.* **1985**, *107*, 7304.
(11) Heatley, F. *Prog. Nucl. Magn. Reson. Spectrosc.* **1979**, *13*, 47.
(12) Connor, T. M. *Trans. Faraday Soc.* **1964**, *60*, 1574.
(13) Schaefer, J. *Macromolecules* **1973**, *6*, 882.
(14) Valeur, G.; Jarry, J. P.; Geny, F.; Monnerie, L. J. *Polym. Sci., Polym. Phys. Ed.* **1975**, *13*, 667, 675, 2251.
(15) Jones, A. A.; Stockmeyer, W. H. *J. Polym. Sci., Polym. Phys. Ed.* **1977**, *15*, 1347.
(16) Hall, C. K.; Helfand, E. *J. Chem. Phys.* **1982**, *77*, 3275.
(17) Helfand, E. *J. Chem. Phys.* **1971**, *54*, 4651.
(18) Kramers, H. A. *Physica* **1940**, *7*, 284.
(19) Dewar, M. J. S.; Zocbisch, E. G.; Healy, E. F. *J. Am. Chem. Soc.* **1985**, *107*, 3902.
(20) Frisch, M. J.; Trucks, G. W.; Head-Gordon, M.; Gill, P. M. W.; Wong, M. W.; Foresman, J. B.; Johnson, B. G.; Schlegel, H. B.; Robb, M. A.; Replogle, E. S.; Gomperts, R.; Andres, J. L.; Raghavachari, K.; Binkley, J. S.; Gonzalez, C.; Martin, R. L.; Fox, D. J.; Baker, J.; Stewart, J. J. P.; Pople, J. A. *Gaussian 92*, revision E.3; Gaussian Inc.: Pittsburgh, PA, 1992.
(21) Matsuzaki, K.; Kanai, T.; Matsubara, T.; Matsumoto, S. *J. Polym. Sci., Polym. Chem. Ed.* **1976**, *14*, 1475.
(22) Brigodiot, M.; Cheradame, H.; Fontanille, M.; Vairon, J. P. *Polymer* **1976**, *17*, 254.
(23) Riseman, J.; Kirkwood, J. G. *J. Chem. Phys.* **1949**, *16*, 442.
(24) Ishihara, A. *Adv. Polym. Sci.* **1958**, *5*, 531.
(25) Dejean de la Batie, R.; Laupretre, F.; Monnerie, L. *Macromolecules* **1988**, *21*, 2052.
(26) Dejean de la Batie, R.; Laupretre, F.; Monnerie, L. *Macromolecules* **1989**, *22*, 122.
(27) Dejean de la Batie, R.; Laupretre, F.; Monnerie, L. *Macromolecules* **1989**, *22*, 2617.
(28) Radiotis, T.; Brown, G. R.; Dais, P. *Macromolecules* **1993**, *26*, 1445.
(29) Dais, P.; Nedea, M. E.; Morin, F. G.; Marchessault, R. H. *Macromolecules* **1990**, *23*, 3387.
(30) Howarth, O. W. *J. Chem. Soc., Faraday Trans. 2* **1979**, *75*, 863.
(31) Denault, J.; Prud'homme, J. *Macromolecules* **1989**, *22*, 1307.
(32) Mashimo, S. *Macromolecules* **1976**, *9*, 91.
(33) Glowinkowski, S.; Gisser, D. J.; Ediger, M. D. *Macromolecules* **1990**, *23*, 3520.
(34) Connolly, J. J.; Gordon, E.; Jones, A. A. *Macromolecules* **1984**, *17*, 222.
(35) Jones, A. A. *J. Polym. Sci., Polym. Phys. Ed.* **1977**, *15*, 863.
(36) Ghesquiere, D.; Ban, B.; Chachaty, C. *Macromolecules* **1977**, *10*, 743.
(37) Wittebort, R. J.; Szabo, A. *J. Chem. Phys.* **1978**, *69*, 1722.
(38) Gronski, W.; Murayama, N. *Makromol. Chem.* **1978**, *179*, 1521.

MA945009Y